

# Propagation Delay-Aware Unslotted Schedules With Variable Packet Duration for Underwater Acoustic Networks

Prasad Anjangi, *Student Member, IEEE*, and Mandar Chitre, *Senior Member, IEEE*

**Abstract**—Recent advances in scheduling transmissions for underwater acoustic networks utilize and exploit long propagation latency of acoustic waves for achieving throughput gain. These techniques utilize the propagation delay information of the considered network geometry and schedule transmissions in time slots. Time-slotted transmissions are such that most of the interference overlaps with the transmission slots and the receiving slots are interference free. Moreover, exploiting propagation delays lead to multiple transmissions per time slot, thereby resulting in higher throughput. However, the packet duration of each transmission in the time slot is assumed to be fixed. The packet duration, however, provides a degree of freedom that, if utilized, results in strategies that can be adopted to achieve throughput closer to the established upper bound. Therefore, we consider the problem of finding unslotted transmission schedules allowing unequal packet duration. Given the propagation delay between nodes in the network and packet traffic demands, we formulate an optimization problem for minimizing the fractional idle time in a frame (or period) of the schedule as a mixed-integer linear fractional problem (MILFP). We compare our results to the recent advancements that exploit large propagation delays and result in time-slotted and unslotted schedules with fixed packet duration. We also present schedules computed for various network geometries with arbitrary packet traffic demands.

**Index Terms**—Underwater acoustic networks, packet traffic demand, scheduling, throughput.

## I. INTRODUCTION

UNDERWATER acoustic (UWA) networks are increasingly gaining attention in the areas of ocean exploration, marine research, commercial marine applications, offshore oil industries, etc. [1]–[4]. Despite the technological advances in UWA communications and networking, medium access control (MAC) is still a challenging problem due to the large propagation delay of the acoustic channel and the half-duplex nature of communication links. The propagation speed of sound underwater is roughly five orders of magnitude lower than that of radio waves in air [5]. While propagation delay is negligible for terrestrial radio-frequency (RF) communications, it is an impor-

tant parameter to be considered in the design of MAC protocols for UWA communications. Due to the presence of such unique characteristics in UWA channels, MAC protocols designed for terrestrial wireless networks cannot be directly adopted [2], [6].

Efficient scheduling and resource allocation are essential components for enabling throughput maximization in wireless networks adopting contention-free MAC protocols. The class of contention-free protocols includes code division multiple access (CDMA), frequency division multiple access (FDMA), and time division multiple access (TDMA). These protocols divide the available channel capacity in the acoustic channel into a set of logical channels for the purpose of multiple access. Among these protocols, FDMA is considered inefficient for underwater applications [7]. Most of the work has focused on CDMA- and TDMA-based protocols. An advantage of TDMA-based protocols is that they provide flexibility in terms of implementation over any physical layer technology. However, in the case of CDMA, the available physical layer resources, such as bandwidth and power, must be divided among the users. Moreover, for designing time domain interference alignment schemes by exploiting large propagation delays, TDMA is a perfect fit. TDMA-based protocols have been studied in [8]–[20] and more recently in [10]–[15], [19], and [20]. In TDMA-based protocols, the time is partitioned into slots and in each time slot, a node can take a decision to either transmit or remain idle based on the objective being optimized. The time slots are further grouped into a frame and these frames repeat periodically.

A variety of scheduling approaches have been proposed that mitigate the effect of large propagation delays to improve the overall system performance, e.g., [9] and [16]–[18]. The best performance achieved using these techniques is comparable to wireless networks with negligible propagation delays. The presence of large propagation delay relative to the packet duration provides a unique opportunity of multiple packets concurrently propagating in the underwater channel, which must be exploited in order to improve the channel utilization. A fundamental understanding of the potential of exploiting large propagation delays in UWA networks to allow network throughput beyond that of networks with negligible propagation delays is provided in [12].

Various objectives including maximizing the number of transmission opportunities [12], minimizing the interference burden [15], and minimizing the schedule length [13] have been

Manuscript received December 31, 2015; revised July 4, 2016 and September 18, 2016; accepted December 3, 2016.

Associate Editor: M. Stojanovic.

The authors are with the Department of Electrical and Computer Engineering, National University of Singapore, Singapore 119227, Singapore (e-mail: prasad.anjangi@u.nus.edu; mandar@arl.nus.edu.sg).

Digital Object Identifier 10.1109/JOE.2016.2637098

considered for finding schedules exploiting large propagation delays. In [12], Chitre *et al.* present a technique to design transmission schedules that ensure most of the interfering messages overlap in time at the unintended receivers, and the desired messages are interference free at the intended receivers. A closely related work is presented in [14], where Lmai *et al.* use similar techniques as in [12], and establish an upper bound on throughput for multihop grid UWA networks and present the schedules which, when adopted, achieve the throughput upper bound. A subsequent work presenting the potential of exploiting propagation delay in scheduling for multihop UWA networks was presented in [15]. Zeng *et al.* [15] develop a distributed scheduling algorithm which follows the same principle of time domain interference alignment as presented in [12], i.e., the scheduling constraints make sure that the messages from the intended transmitter can be received free of interference while the interfering messages from its unintended transmitters can maximally overlap. The optimal throughput is computed for a smaller number of links scheduled in the network. However, the scheduling feasibility constraints do not consider the interframe collisions due to which the times at the end of the frame are underutilized and can cause inefficiency. This problem is addressed in [13]. The authors formulate the scheduling problem as a mixed-integer linear problem (MILP) and consider the intraframe as well as interframe scheduling constraints. This allows for a better efficiency as it avoids the collisions among adjacent frames and thereby results in a smaller frame length and higher throughput. However, the objective minimized in [13] is the frame length and the packet duration is fixed. Although multiple transmissions per link are considered, the packet duration is not a variable in the MILP considered in [13]. We observe that even if the packet duration is considered a variable in the MILP minimizing the frame length it results in schedules in which the packet duration of all transmissions remains same and is equal to the lower bound set on the packet duration. Hence, minimizing the frame length constrains the full exploitation of the long propagation delays in UWA networks as it always results in equal packet duration. The packet duration provides a degree of freedom that, if utilized, provides schedules with throughput much higher as compared to those achievable using state-of-the-art methods available and is closer to the upper bound  $\frac{N}{2}$  [12, Th. 1], where  $N$  is the number of nodes in the network. The specific contributions of this paper are as follows.

- 1) We formulate a TDMA-based scheduling problem as an MILFP which better exploits long propagation delays in static UWA networks. We consider minimizing the total fractional idle time in a frame which allows for multiple concurrent transmissions in the medium. The solution results in the schedule with variable packet lengths.
- 2) We show that the proposed centralized algorithm resulting in unslotted and variable packet length schedules performs better than other state-of-the-art centralized algorithms available for computing optimal schedules. Specifically, we compare our results to the following techniques:
  - a) the time-slotted fixed packet duration schedules that are computed using centralized algorithm proposed in [12];
  - b) the unslotted fixed packet duration schedules that are computed using centralized algorithm proposed in [13].

- 3) We consider some network geometries for which the optimal schedules are known from [12] and present the schedules when arbitrary packet traffic demands are to be satisfied on each link. The throughput drops in many cases but still remains more than 1. Moreover, it demonstrates the capability of the algorithm to compute transmission schedules with different packet traffic demands.
- 4) The large propagation delay is relative to the transmitted packet duration and hence we quantify the values and show the regions in which the considered networks must be operated to achieve significant throughput gains when compared to radio-frequency-based terrestrial wireless networks with negligible propagation delays.

The rest of the paper is organized as follows. In Section II, we present the system model and assumptions. The problem is formulated and the MILFP optimization is set up in Section III. This is followed by the parametric algorithm to solve MILFP in Section IV. In Section V, we consider a realistic network geometry from a sea-trial experiment and demonstrate the throughput gain. The computed optimal schedules for network geometries with arbitrary packet traffic demands are shown in Section VI. The scalability and complexity analysis of the proposed MILFP algorithm is presented in Section VII. The regions of operation for the UWA network where the throughput gains can be achieved are presented in Section VIII and finally the conclusions are drawn in Section IX.

## II. SYSTEM MODEL AND ASSUMPTIONS

The system model and assumptions are as follows.

- 1) A set  $\mathcal{L}$  of directed links is considered for scheduling in a UWA network, given the propagation delay between all nodes in the network and traffic demands on each link  $l \in \mathcal{L}$ . Each link  $l$  can be explicitly written as a 2-tuple  $(j, k)$  which represents a link where node  $j$  is the transmitter and node  $k$  is the receiver. The propagation delay corresponding to link  $(j, k)$  is  $D_{jk}$  in seconds. The packet traffic demand  $\Lambda_{jk}$  for link  $(j, k)$  is defined as the number of packets to be transmitted in a single frame on link  $(j, k)$ .
- 2) We allow having packets of different lengths for the same link. The time relative to the start of the frame, at which node  $j$  starts transmitting the  $x$ th packet to node  $k$  is  $t_{jk}^x$ , where  $x \in \{1, \dots, \Lambda_{jk}\}$ . The packet/transmission duration corresponding to the  $x$ th transmission on link  $(j, k)$  is  $\tau_{jk}^x$ . The frame length of the schedule (also termed as period of the schedule in [12]) is  $T$ .
- 3) A central controller computes schedules based on the available information on the network topology and traffic demands while exploiting the large propagation delay between the nodes. The network considered is static (with small motion around the location at which nodes are deployed). The centralized optimal solution provides an upper bound on the performance of any distributed

or heuristic algorithm due to limited knowledge of the network topology in case of the former and dependence on the quality of heuristic in the case of latter. Such an upper bound allows evaluation of the performance of distributed and heuristic algorithms. For example, the recent distributed algorithms proposed in [15], [22], and [21] can be compared against such an upper bound.

- 4) The mathematical formulation allows having packets of different lengths for the same link. We assume link traffic demands to be given in the case of the single-hop networks or are calculated by given end-to-end traffic demands in case of a multihop network with predetermined routing. The proposed framework may be extended to include routing in the optimization problem, but this is out of the scope of this paper.
- 5) We consider a form of TDMA as in several recent works [12]–[15]. We partition time into frames but do not further partition into slots as commonly done. This problem formulation allows us to have variable packet duration for each transmission with no slotting required. This plays an important role in achieving throughput gain. The objective considered for minimization is the fractional idle time in a frame. The idle time is the total time for which the nodes are neither transmitting nor receiving.
- 6) Underwater acoustic modems are assumed to be half-duplex in nature, i.e., a node cannot receive and transmit simultaneously. All the transmissions are assumed to be unicast and intended to their corresponding destinations, i.e., a node cannot receive from or transmit to more than one node simultaneously.
- 7) We adopt a protocol channel model [23] and denote by  $\alpha$  the ratio of interference range to the communication range. The protocol channel model assumes that, if two packets partially overlap in time at the receiver node, then the receiver is unable to receive either packet successfully. The communication range depends on the transmission power at the transmitting nodes. If the transmission power is set such that the communication range is greater than or equal to the size of the network considered, any transmission on a particular node is heard by all other nodes in the network resulting in the single collision domain, although note that in multihop networks, the communication range, and the corresponding interference range will not include all the nodes in the network and might result in multiple partially overlapping collision domains.
- 8) The propagation delay corresponding to the maximum interference range in the network considered is denoted by  $G$  and is given by

$$G = \max_{i,j} \alpha D_{ij} \quad (1)$$

where  $i, j \in \{1, \dots, N\}$ .

### III. PROBLEM FORMULATION

Consider a pair of links  $(j, k), (l, i) \in \mathcal{L}$  such that node  $j$  transmits its  $x$ th packet to node  $k$  and node  $l$  transmits its  $y$ th packet to node  $i$  (see Fig. 1). Fig. 1 illustrates the effect of

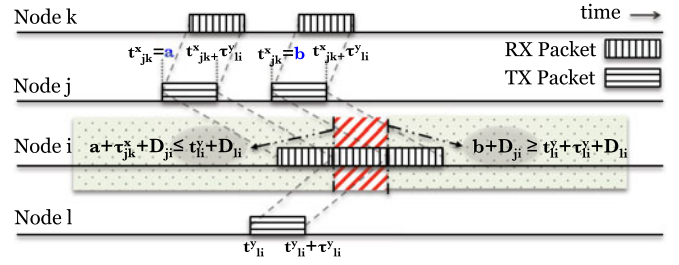


Fig. 1. Illustration of the effect of propagation delay on transmission times of packets to be transmitted on links  $(j, k)$  and  $(l, i)$ .

propagation delay. The interference is caused at node  $i$ , only if node  $j$  transmits at such a time  $t_{jk}^x$  that it ends up in the hatched region (in red) marked in Fig. 1 at node  $i$ . The choice of  $t_{jk}^x \leq a$  or  $t_{jk}^x \geq b$  avoids the interference during reception time at node  $i$  and ends up in the dotted region (in green) instead. Note that the packet lengths  $\tau_{jk}^x$ 's and  $\tau_{li}^y$  are considered equal in Fig. 1 only for the purpose of illustration. For node  $j$ 's transmission to not interfere with node  $i$ 's reception, either of the following necessary conditions needs to be satisfied:

$$t_{jk}^x + \tau_{jk}^x + D_{ji} \leq t_{li}^y + D_{li} \quad (2)$$

or

$$t_{jk}^x + D_{ji} \geq t_{li}^y + \tau_{li}^y + D_{li} \quad (3)$$

$\forall \{(j, k), (l, i) \in \mathcal{L} | D_{ji} \leq \alpha D_{jk}\}$ , where the condition  $D_{ji} \leq \alpha D_{jk}$  is satisfied when node  $i$  lies in the interference range of node  $j$ . The transmission start times  $t_{jk}^x, t_{li}^y$  and corresponding packet duration  $\tau_{jk}^x, \tau_{li}^y$  must be chosen such that the desired message at node  $i$  is interference free. The conditions stated in (2) and (3) are illustrated in Fig. 1. Note that if the interference range is larger than the size of the network considered (single collision domain network), then each transmission in the network is heard by all the nodes. In this case, the conditions in (2) and (3) apply to all the links in  $\mathcal{L}$ . We consider single collision domain network throughout, since this model allows us to study the effects of propagation delay for the worst case scenario, although the formulation is general enough to be used for both single-hop as well as multihop UWA networks. While presenting the scalability analysis in Section VII, we consider a multihop network with multiple partially overlapping collision domains.

If the transmission scheduling decisions are taken considering the propagation-delay-based constraints listed in (2) and (3), the corresponding receptions at the nodes will be interference free, i.e., there will be no collisions within a frame. However, note that the following possibilities are not captured in the constraints listed in (2) and (3):

- 1) the transmissions from the previous frames interfering with reception in the current frame;
- 2) the transmission in the current frame interfering with possible reception in the subsequent frames.

Not considering the above conditions will result in poor schedules. To consider the interframe constraints, we generalize

the inequalities

$$t_{jk}^x + \beta T + \tau_{jk}^x + D_{ji} \leq t_{li}^y + D_{li} \quad (4)$$

or

$$t_{jk}^x + \beta T + D_{ji} \geq t_{li}^y + \tau_{li}^y + D_{li} \quad (5)$$

$\forall \{(j, k), (l, i) \in \mathcal{L}\}$ , where  $\beta \in \mathbb{Z}$  is the integer constant which determines the number of adjacent frames in the past and future in time that are considered. Note that setting  $\beta = 0$  in (4) and (5) leads to (2) and (3), respectively.  $\beta = -1$  corresponds to conditions considering one adjacent frame in the past while  $\beta = 1$  corresponds to conditions considering one adjacent frame in the future.

There is no upper bound on the value of  $\beta$ , since the frame length can be arbitrarily small theoretically. In practice, the schedules with such smaller frame lengths are not implementable on underwater modems for practical use. In [12], the optimal schedules for the network geometries result in the frame lengths which are at least greater than  $G$ . With this reasonable assumption of limiting the value of frame length to be greater than the girth of the network  $T > G$ , we limit our constraints to  $\beta = 0$ ,  $\beta = 1$ , and  $\beta = -1$ . Consider the transmission of a packet in current frame at time  $t$  for duration  $\tau$ . Interference caused due to this transmitted packet in worst case only lasts until time  $t + G + \tau$ . Since we know  $G < T$ , we have  $t + G + \tau < t + T + \tau \Rightarrow t + G < t + \beta T, \beta = 1$ . In other words, in the worst case scenario, the interference is only limited within the next frame.

#### A. Propagation-Delay Constraints

Consider scheduling all links  $(j, k) \in \mathcal{L}$  in a frame. The number of packets to be transmitted on each link  $(j, k)$  is given by the traffic demand for that link  $\Lambda_{jk}$  packets/frame.  $x$  is the index associated with link  $(j, k)$  taking values  $1, \dots, \Lambda_{jk}$  and similarly  $y$  is the index for link  $(l, i)$  taking values  $1, \dots, \Lambda_{li}$  (e.g.,  $t_{jk}^1, \dots, t_{jk}^{\Lambda_{jk}}, \tau_{jk}^1, \dots, \tau_{jk}^{\Lambda_{jk}}$  are variables associated with transmission time and packet duration for each link  $(j, k)$ ). Note that the conditions listed in (4) and (5) form a set of disjunctive constraints which results in the feasible set forming a nonconvex region over which the search for the solution is required. There are two well-known methods for conversion of disjunctive constraints to conjunctive constraints: convex-hull reformulation [24] and Big- $M$  reformulation [25], [26]. We use the Big- $M$  transformation to convert the disjunctive constraints (4) and (5) into conjunction and rearrange them as following:

1)  $\beta = 0$

$$t_{jk}^x - t_{li}^y + \tau_{jk}^x \leq -(D_{ji} - D_{li}) + Mp_{jk,li}^{xy} \quad (6)$$

$$-t_{jk}^x + t_{li}^y + \tau_{li}^y \leq (D_{ji} - D_{li}) + M(1 - p_{jk,li}^{xy}); \quad (7)$$

2)  $\beta = 1$

$$t_{jk}^x - t_{li}^y + \tau_{jk}^x + T \leq -(D_{ji} - D_{li}) + Mq_{jk,li}^{xy} \quad (8)$$

$$-t_{jk}^x + t_{li}^y + \tau_{li}^y - T \leq (D_{ji} - D_{li}) + M(1 - q_{jk,li}^{xy}); \quad (9)$$

3)  $\beta = -1$

$$t_{jk}^x - t_{li}^y + \tau_{jk}^x - T \leq -(D_{ji} - D_{li}) + Mr_{jk,li}^{xy} \quad (10)$$

$$-t_{jk}^x + t_{li}^y + \tau_{li}^y + T \leq (D_{ji} - D_{li}) + M(1 - r_{jk,li}^{xy}); \quad (11)$$

where  $p_{jk,li}^{xy}, q_{jk,li}^{xy}$  and  $r_{jk,li}^{xy}$  are the binary variables<sup>1</sup> associated with each pair of disjunctive constraints considered  $\forall (j, k), (l, i) \in \mathcal{L}$  and  $x \in \{1, \dots, \Lambda_{jk}\}, y \in \{1, \dots, \Lambda_{li}\}$ . Inequalities (4) and (5) are presented in (6)–(11) after the Big- $M$  transformation for the values of  $\beta$  from the set  $\{-1, 0, 1\}$ .

#### B. Duration Between Two Consecutive Transmissions

Since the packet traffic demands  $\Lambda_{jk}$  packets per frame for link  $(j, k)$ , the following constraint on transmissions from node  $j$  ensures the difference between two consecutive packet transmission times is at least greater than the previous transmitted packet duration:

$$t_{jk}^{x+1} - t_{jk}^x \geq \tau_{jk}^x. \quad (12)$$

#### C. Allowing Transmissions and Receptions Across Frame Boundary

A packet transmission in the current frame at time  $t_{jk}^x$  in the worst case can cause interference until time  $t_{jk}^x + G + \tau_{jk}^x$ . To prevent the end of the packet transmission on the link causing maximum interference in future to cross the subsequent frame, we impose the following constraint:

$$t_{jk}^x + G + \tau_{jk}^x < 2T. \quad (13)$$

Note that the above constraint does not restrict the transmissions in the frame to be fully contained within the frame.

#### D. Throughput

The average throughput  $S$  of a schedule with frame length  $T$  can be computed by summing the total reception (or equivalently transmission) time on all the nodes in the network in one frame duration  $T$

$$S = \frac{1}{T} \sum_{j=1}^N \left[ \sum_{(k,j) \in \mathcal{L}} \sum_{x=1}^{\Lambda_{kj}} \tau_{kj}^x \right]. \quad (14)$$

#### E. Inclusion of Packet Headers

In practical modems, the packet consists of the header and payload. We can include the packet headers in the problem formulation by replacing  $\tau_{jk}^x$  with  $\overline{\tau}_{jk}^x$  in all constraints except the objective function, where

$$\overline{\tau}_{jk}^x = \tau_p + \tau_{jk}^x \quad (15)$$

<sup>1</sup> With the binary variable taking value 0 or 1 (e.g.,  $p_{jk,li} = 0$  or 1) along with a large enough value of parameter  $M$ , one of the constraints in the disjunctive pair becomes redundant. Note that the smaller the value of  $M$ , the tighter the Big- $M$  reformulation can be. We select an arbitrarily large value of  $M$  for the transformation.



TABLE I  
SUMMARY OF NOTATIONS AND PARAMETERS

Variable	Description
$(j, k)$	A directed link with node $j$ as transmitter and node $k$ as receiver
$(l, i)$	A directed link with node $l$ as transmitter and node $i$ as receiver
$\mathcal{L}$	Set of all links in the network
$D_{jk}$	Propagation delay corresponding to link $(j, k)$
$\Lambda_{jk}$	The number of packets to be transmitted on link $(j, k)$ in a single frame
$t_{jk}^x$	Transmission time of the $x^{\text{th}}$ packet scheduled on link $(j, k)$
$t_{li}^y$	Transmission time of the $y^{\text{th}}$ packet scheduled on link $(l, i)$
$\tau_{jk}^x$	Transmission/Packet duration of the $x^{\text{th}}$ packet scheduled on link $(j, k)$
$\tau_{li}^y$	Transmission/Packet duration of the $y^{\text{th}}$ packet scheduled on link $(l, i)$
$t_p$	Packet header duration
$\tau_{lb}$	Lower bound on the packet duration on all links
$\alpha$	Ratio of interference range to communication range
$p_{jk,li}^{xy}, q_{jk,li}^{xy}, r_{jk,li}^{xy}$	Binary variables associated with each pair of variables $t_{jk}^x$ and $t_{li}^y$ for the Big-M transformation
$T$	Frame duration
$\beta$	Number of adjacent frames in the past and future considered for collisions due to propagation delay
$G$	Propagation delay corresponding to the maximum interference range in the network
$S$	Normalized network throughput

and  $t_p$  is the packet header duration whereas  $\tau_{jk}^x$  is the payload duration. We present the results including the nonnegligible packet headers in Section V-A3.

### F. Objective Function

The objective considered in the recent work [13] is to minimize the frame length  $T$ , and the packet duration is fixed. Even if the packet duration is considered a variable, minimizing  $T$  results in packet duration which are equal in size for all transmissions to the lower bound set on the packet duration. We demonstrate this in Section V for a particular case. Minimizing  $T$  prevents the full exploitation of large propagation delays in UWA networks. To utilize the degree of freedom that is provided by varying the packet duration, we formulate a different objective which results in variable packet duration and eventually a significant gain in throughput. We know that the throughput upper bound is  $\frac{N}{2}$  from [12], i.e.,

$$S \leq \frac{N}{2} \Rightarrow N - 2S \geq 0 \quad (16)$$

$$\Rightarrow \frac{NT - 2 \sum_{j=1}^N \left[ \sum_{(k,j) \in \mathcal{L}} \sum_{x=1}^{\Lambda_{kj}} \tau_{kj}^x \right]}{T} \geq 0. \quad (17)$$

The numerator in the resulting equation shown in (17) is split into three terms to show that it results in fractional idle time in a frame as shown in (18). Note that the minimization of fractional idle time results in maximal usage of the total time available in a frame and allows for multiple nodes to transmit simultaneously without causing collisions. The objective function to be minimized as the fractional idle time in a frame is

$$f_{\text{MILFP}} = \frac{1}{T} \left[ NT - \underbrace{\sum_{j=1}^N \left\{ \sum_{(j,k) \in \mathcal{L}} \sum_{x=1}^{\Lambda_{jk}} \tau_{jk}^x \right\}}_{\text{sum of TX Packet duration from Node } j} + \underbrace{\sum_{(k,j) \in \mathcal{L}} \sum_{x=1}^{\Lambda_{kj}} \tau_{kj}^x}_{\text{sum of RX Packet duration at Node } j} \right] \quad (18)$$

where  $N$  is the total number of nodes in the network. The first term of the numerator in (18) is the sum of the total time available including all the  $N$  nodes in the network per frame. The rest comprises two terms which constitute the amount of time the network nodes are busy with transmissions and receptions. The frame length  $T$  in the denominator of (18) prevents the frame length from taking very small values resulting in trivial solutions. The objective function in (18) is a ratio of two linear functions. This is a nonlinear objective function and together with the mixed-integer propagation-delay constraints the problem is an MILFP [27]

$$\begin{aligned} \min \quad & \frac{1}{T} \left[ NT - \sum_{j=1}^N \left\{ \sum_{(j,k) \in \mathcal{L}} \sum_{x=1}^{\Lambda_{jk}} \tau_{jk}^x + \sum_{(k,j) \in \mathcal{L}} \sum_{x=1}^{\Lambda_{kj}} \tau_{kj}^x \right\} \right] \\ \text{s.t.} \quad & t_{jk}^x - t_{li}^y + \tau_{jk}^x - Mp_{jk,li}^{xy} \leq -(D_{ji} - D_{li}) \\ & -t_{jk}^x + t_{li}^y + \tau_{li}^y + Mp_{jk,li}^{xy} \leq (D_{ji} - D_{li}) + M \\ & t_{jk}^x - t_{li}^y + \tau_{jk}^x + T - Mq_{jk,li}^{xy} \leq -(D_{ji} - D_{li}) \\ & -t_{jk}^x + t_{li}^y + \tau_{li}^y - T + Mq_{jk,li}^{xy} \leq (D_{ji} - D_{li}) + M \\ & t_{jk}^x - t_{li}^y + \tau_{jk}^x - T - Mr_{jk,li}^{xy} \leq -(D_{ji} - D_{li}) \\ & -t_{jk}^x + t_{li}^y + \tau_{li}^y + T + Mr_{jk,li}^{xy} \leq (D_{ji} - D_{li}) + M \\ & -t_{jk}^{x+1} + t_{jk}^x + \tau_{jk}^x \leq 0 \\ & t_{jk}^x + \tau_{jk}^x - 2T < -G. \end{aligned} \quad (19)$$

The domains of the variables in the above optimization problem are  $t_{jk}^x, T \in \mathbf{R}^+$  and  $p_{jk,li}^{xy}, q_{jk,li}^{xy}, r_{jk,li}^{xy} \in \{0, 1\} \quad \forall j, k, l, i \in \{1, \dots, N\}, (j, k), (l, i) \in \mathcal{L}, x \in \{1, \dots, \Lambda_{jk}\}, y \in \{1, \dots, \Lambda_{li}\}$  and  $\tau_{lb} \leq \tau_{jk}^x \leq \infty$ , where  $\tau_{lb} \in \mathbf{R}^+$  is the lower bound set on the packet duration. The notations and parameters used in this formulation are summarized in Table I. This formulation does not restrict the packet duration from being zero. This might lead to unfair distribution of time with most time being assigned to the nodes in the network such that the throughput is maximized. To ensure some link fairness, a lower bound  $\tau_{lb}$

**Algorithm 1:** Parametric Algorithm.**Initialization.**Set  $n = 1$ ,  $w_1 := 0$ ,  $\epsilon = 10^{-4}$ **for**  $n = 1, 2, \dots$  **do**

Solve equivalent sub-problem

 $F(w) = \min \left\{ \mathbf{c}^T \mathbf{x} + \mathbf{d} - w_n (\mathbf{e}^T \mathbf{x} + f) \right\}$  subject to constraints in (19)**if**  $|F(w_n)| \geq \epsilon$  **then**let  $w_{n+1} = \frac{\mathbf{c}^T \mathbf{x}_n^* + \mathbf{d}}{\mathbf{e}^T \mathbf{x}_n^* + f}$ **else**Stop, output  $\mathbf{x}_n^*$  as optimal solution and  $w^* = w_n$  as the optimal value**end if****end for**

on the packet duration for any transmission on link  $(j, k)$  can be set to a nonzero value. This ensures that node  $j$  transmits to node  $k$  at least  $\Lambda_{jk} \tau_{lb}$  s per frame.

Propagation delays considered in this formulation are assumed to be known with absolute certainty. However, we can consider uncertainties in propagation delays due to reasons such as node mobility because of ocean currents, uncertainty in the measurement of exact deployed locations, and physical changes in the ocean environment. We can model the uncertainty or variation in the propagation delay by assuming that they are known to lie in a given set. The formulated optimization problem (19) can be modified and reformulated as a robust optimization problem [28] to find the optimal schedule which is robust to all those values of propagation delays lying in the uncertainty set considered.

## IV. MILFP SOLUTION

An MILFP has an objective function which is a ratio of two linear functions subject to mixed-integer linear constraints. The parametric algorithm based on Newton's method has been recently proposed as an efficient solution method to MILFP problems [27], [29]. For the sake of brevity, let us denote the objective function in (18), which is a ratio of two linear functions, in a concise form as

$$f_{\text{MILFP}} = \frac{1}{T} \left[ NT - \sum_{j=1}^N \left\{ \sum_{(j,k) \in \mathcal{L}} \sum_{x=1}^{\Lambda_{jk}} \tau_{jk}^x + \sum_{(k,j) \in \mathcal{L}} \sum_{x=1}^{\Lambda_{kj}} \tau_{kj}^x \right\} \right] \\ = \frac{\mathbf{c}^T \mathbf{x} + \mathbf{d}}{\mathbf{e}^T \mathbf{x} + f} \quad (20)$$

where  $\mathbf{x}$  is the vector of variables and  $\mathbf{c}, \mathbf{e}$  are coefficients in the fractional linear objective.

The main idea of this algorithm is to transform the original MILFP problem into an equivalent parametric MILP problem  $F(w)$  as shown in Algorithm 1. This problem has the same constraints but a different objective function formulated as the numerator of the original objective function minus the denominator multiplied by a parameter  $w$ . One unique feature of the function  $F(w)$  is that when  $F(w) = 0$ , the inner MILP



Fig. 2. UNET network node locations during the MISSION 2013 experiment (deployment #1). White markers are network nodes. The geometry considered for the case study is marked with the distances between the links.

problem has a unique optimal solution which is exactly the same as the global optimal solution to the original MILFP problem [29]. Based on this property of  $F(w)$ , solving the MILFP problem becomes equivalent to finding the root of the equation  $F(w) = 0$ . Therefore, numerical root-finding approaches such as Newton's method can be applied to solve this problem.

## V. RESULTS

To demonstrate throughput gain, we first consider a realistic network geometry from an at-sea experiment and then show the average throughput gain computed over several random three node network deployments. To show the throughput gain that can be achieved by packet duration variability, we present a comparative study between the following methods.

- 1) Time-slotted fixed packet duration solution—In this approach, we compute the time-slotted transmission schedule to be used with optimal time slot length and packet duration minimizing the guard times. We use the algorithm presented in [12] to compute the throughput optimal schedule for the considered network geometry.
- 2) Unslotted fixed packet duration solution—For this case, we consider the MILP algorithm presented in [13] and compute throughput at the optimal value of packet duration which is an unslotted schedule with the least frame length.
- 3) Variable packet duration with no time slotting solution—In this case, we solve the MILFP shown in (19), which minimizes the fractional idle time in a frame, using Algorithm 1 and calculate the throughput.

## A. Throughput Gain: Sea-Trial Network Geometry

The UNET network deployed (Fig. 2) during the MISSION 2013 experiment in Singapore waters consisted of a UNET-II modem [30] (marked P21 in Fig. 2) mounted below a barge and six UNET-PANDA nodes [31] deployed at various locations within  $2\text{-km} \times 2\text{-km}$  area around the barge. The modems labeled as P21, P28, and P29 in Fig. 2 are node 1, node 2, and node 3, respectively, in the analysis. Given this network geometry, we schedule the links in

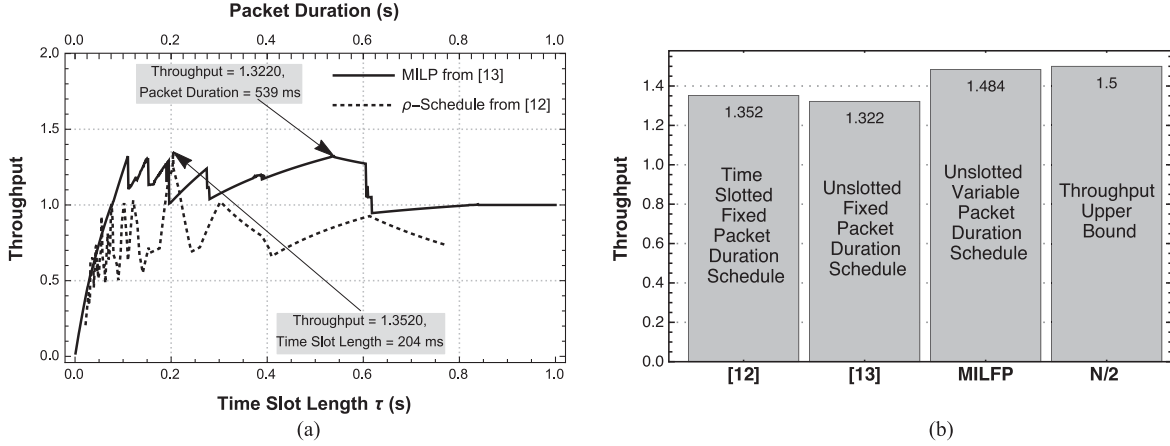


Fig. 3. Throughput sensitivity to time slot length while using the algorithm in [12] and to packet duration while using the algorithm in [13] is shown along with the throughput comparison when using the proposed MILFP technique resulting in unslotted variable packet duration schedules for the considered sea-trial network geometry. (a) Throughput sensitivity to time slot length and packet duration. (b) Throughput comparison of centralized algorithms.

$\mathcal{L} = \{(1, 2), (2, 1), (2, 3), (3, 2), (1, 3), (3, 1)\}$ . The corresponding propagation delays are computed considering the speed of sound underwater  $c = 1540$  m/s. For the considered network geometry, the distances among the nodes are marked as shown in Fig. 2.

1) *Time-Slotted Fixed Packet Duration Solution:* To compute the schedules using the algorithm presented in [12], we require the propagation delay between links in units of time slot length. Moreover, the algorithm in [12] only accepts integer propagation delays. We present some preliminary concepts and notation required to understand the solution.

The network geometry can be represented in the form of a delay matrix shown in [12, eq. (1)], where each element of the delay matrix contains the propagation delay between the corresponding pair. The delay matrix is denoted by  $\mathbf{D}$  and each of its element  $D_{jk}$  denotes the measured propagation delay between node  $j$  and node  $k$  in units of time slot length  $\tau$ . Note that the elements of the delay matrix can be noninteger, i.e.,  $\mathbf{D}$  can be a noninteger delay matrix. But with appropriate choice of time slot length  $\tau$ , the given noninteger delay matrix can be closely approximated to an integer delay matrix  $\mathbf{D}'$  [12, eq. (4)]. If the network has a noninteger delay matrix, packets transmitted on the time slot boundaries may be received across time slot boundaries. For a noninteger delay matrix  $\mathbf{D}$ , the elements are rounded off to yield an integer delay matrix  $\mathbf{D}'$  and the largest round off errors in approximating  $D_{jk}$ 's to the nearest smaller and larger integer are denoted by  $\rho^+$  and  $\rho^-$ , respectively, and defined in [12, eq. (11)].

Due to the approximations in the delay matrix, the guard intervals are needed at the start and end of the time slots.  $\rho^+$  and  $\rho^-$  are the worst delay approximations made. The packet transmission on the links with these delay approximations will either yield in an early reception of the packet or a delayed reception of the packet depending on whether propagation delay (in units of time slot length  $\tau$ ) of that link is approximated to a larger number or a smaller number, respectively. It is obvious that  $\tau\rho^-$  is the worst amount of time that must be left before the transmission starts in order to prevent the early receptions

TABLE II  
TIME-SLOTTED FIXED PACKET DURATION SOLUTION

Parameter	Value
$\tau^*$	204 ms
$\tau^*(1 - \rho^- - \rho^+)$	184 ms
$t_s$	19.03 ms
$t_e$	0.97 ms
$S_p$	1.35

and  $\tau\rho^+$  is the worst amount of time that must be left after the transmission ends in the time slot, in order to prevent the delayed reception. Hence, we denote these start and end guard times in the time slot by

$$t_s = \tau\rho^- \quad (21)$$

$$t_e = \tau\rho^+. \quad (22)$$

Therefore, the maximum duration for which the time slot can be used for transmission is given by

$$\tau - (t_s + t_e) = \tau(1 - \rho^- - \rho^+). \quad (23)$$

An exhaustive search by varying the time slot length from  $\tau_{\min}$  to  $\tau_{\max}$  in steps of size  $\Delta x$  will provide the optimal time slot length  $\tau$  and guard times  $t_s, t_e$  that can be used.  $\Delta x$  is the smallest incremental duration in the packet length. In practical modems, the step size  $\Delta x$  depends on many factors such as modulation and coding scheme employed at the physical layer. We set  $\Delta x = 1$  ms while performing the exhaustive search. In practice,  $\Delta x$  is usually larger than 1 ms (e.g., in the UNET modem [30]), and hence our throughput estimate here is intentionally optimistic.  $\tau_{\min}$  and  $\tau_{\max}$  are the minimum and maximum possible time slot lengths, the values of which are constrained by the minimum or maximum packet duration that can be set in the underwater acoustic modems. Let  $Z$  denote the number of successful transmissions (or, equivalently, receptions) scheduled in one frame of length  $T$ . For each value of time slot length  $\tau$  between  $\tau_{\min}$  and  $\tau_{\max}$ , the delay matrix and its correspond-

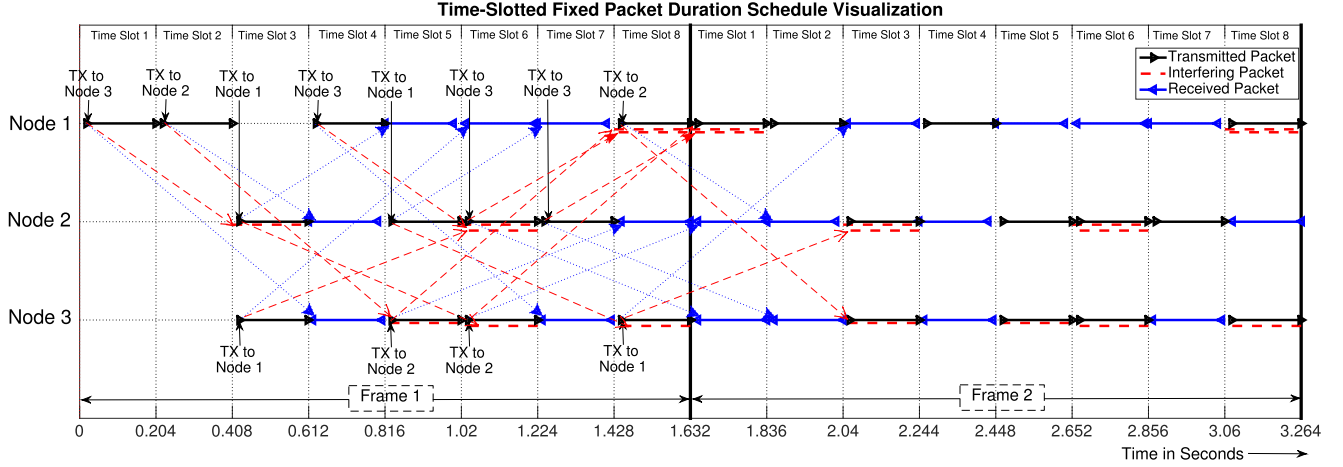


Fig. 4. Schedule visualization with fixed time slot length and packet duration. The guard times set in the time slot take care of the early receptions and delayed receptions problem due to the approximations made in the delay matrix. Throughput achieved is 1.35.

ing approximations  $\rho^+$  and  $\rho^-$  are computed.  $\frac{Z}{T}$  is calculated from the schedule computed using the algorithm from [12]. The throughput  $S_\rho$  is then computed as

$$S_\rho = \frac{Z}{T} \left( \frac{\tau(1 - \rho^- - \rho^+)}{\tau} \right) = \frac{Z}{T} (1 - \rho^- - \rho^+). \quad (24)$$

$S_\rho$  is the number of successful transmissions per time slot multiplied by the time slot efficiency. The time slot length corresponding to the maximum value of the objective function is chosen to be the optimal time slot length  $\tau^*$  and corresponding packet duration is set. Throughput sensitivity to the selection of time slot length is shown in Fig. 3(a) when schedules are computed using algorithm proposed in [12]. Time slot length is varied from 1 to 1000 ms and for those time slot lengths which result in a good approximation to integer delay matrix, the schedule is computed and the corresponding throughput is plotted in the case of [12]. The optimal time slot length and the corresponding throughput are marked in Fig. 3(a).

The time slot length  $\tau$  is varied from  $\tau_{\min} = 1$  ms to  $\tau_{\max} = 1000$  ms and  $\Delta x = 1$  ms is set. The optimal value of time slot length and other parameters are tabulated in Table II. The delay matrix and the integer delay matrix corresponding to time slot length  $\tau^*$  are

$$\mathbf{D} = \frac{\mathbf{L}}{c\tau^*} = \begin{bmatrix} 0 & 1.9067 & 2.9666 \\ 1.9067 & 0 & 3.0048 \\ 2.9666 & 3.0048 & 0 \end{bmatrix}$$

$$\mathbf{D}' = \begin{bmatrix} 0 & 2 & 3 \\ 2 & 0 & 3 \\ 3 & 3 & 0 \end{bmatrix}.$$

With this delay matrix, the optimal schedule is computed using the algorithm presented in [12]. The frame length computed is  $T = 8$  slots with each slot duration  $\tau^* = 204$  ms. The throughput is calculated to be  $S_\rho = 1.35$ . The schedule is visualized in Fig. 4, using the optimal values computed for the network setting. Since we know the time slot length, the guard times, and the frame length of the schedule, we can plot the

TABLE III  
UNSLOTTED FIXED PACKET DURATION SOLUTION

Link	Transmission Start Time (s)	Packet Duration (s)
(1, 2)	3.2676	0.539
(2, 1)	2.0495	0.539
(2, 3)	0.1422	0.539
(3, 2)	0.0683	0.539
(1, 3)	1.3604	0.539
(3, 1)	3.7405	0.539

transmitted packets, the received packets, and the interfered packets accurately in time at each node. We leave  $t_s$  amount of time before the start of the transmission in a transmitting slot and  $t_e$  amount of time at the end of the transmission. In Fig. 4, it is clear that all the receptions are interference free as expected and all interfering packets are aligned with the transmitting slots.

2) *Unslotted Fixed Packet Duration Solution:* In [13], the scheduling problem is formulated as an MILP and the objective function considered for minimization is frame length  $T$ . The packet duration is fixed. To find the optimal packet duration resulting in the maximum throughput we vary the packet duration similar to the time slot length in Section V-A1 in steps of 1 ms. For each value of fixed packet duration set, we compute the schedule and the corresponding throughput. The throughput computed is plotted against the packet duration values and shown in Fig. 3(a). The optimal packet duration and the corresponding throughput are marked in Fig. 3(a). The transmission start times in the schedule at the optimal packet duration are tabulated in Table III. The frame length is  $T = 2.4462$  s. Throughput  $S$  is computed from (14),  $S = 1.3220$ . The optimal schedule computed is visualized in Fig. 5. To visualize the schedule we plot the transmission and reception events in time based on the transmission times, propagation-delay information, and the packet duration computed. Also, note that all the receptions in the schedule shown in Fig. 5 are interference free and most of the interference aligns with the transmission times. The lower bound on the packet duration is set to different values and the



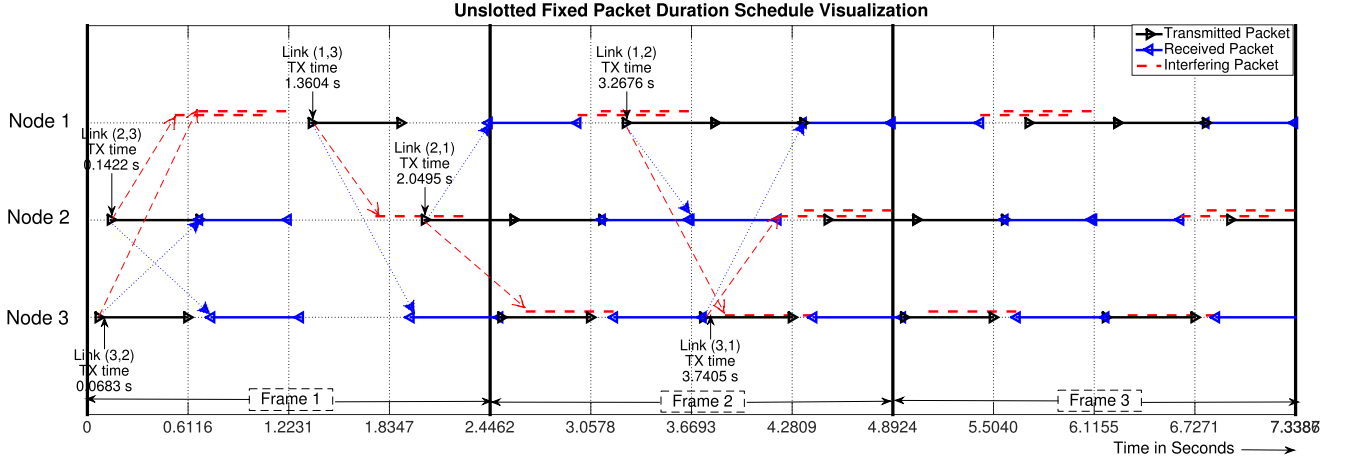


Fig. 5. Schedule visualization for unslotted fixed packet duration schedule. Note that all the packet transmissions are of equal size: 539 ms. Throughput computed is 1.32.

TABLE IV  
VARIABLE PACKET DURATION SOLUTION

Link	Transmission Start Time (s)	Packet Duration (s)
(1, 2)	1.4266	0.7779
(2, 1)	0.9864	0
(2, 3)	0.9864	0.3968
(3, 2)	0.7701	0.4325
(1, 3)	2.2045	0.3968
(3, 1)	0.3890	0.3812

solution still results in all transmissions with equal value, the same as the lower bound set.

Note that even if the packet duration is considered a variable in the MILP in [13], the packet duration values in the resulting solution are equal to the lower bound set on the packet duration. The reason for all the transmission duration to be the same in this case is due to the choice of the objective function which is the frame length  $T$ . If the frame length is minimized, the packet duration of all transmissions contributing to the frame length has to be the least possible values that they can have. Therefore, the frame length is not a good choice if the potential of exploiting the large propagation delays needs to be studied, since this formulation will not allow the variability in the packet duration.

3) *Variable Packet Duration With No Time Slotting Solution:* Next, we consider the solution resulting from solving (19) using Algorithm 1.

- 1) *Uniform packet traffic demand:* The lower bound on packet duration  $\tau_{jk}^x$  is set to 0 and the packet traffic demand considered is 1 packet/frame on each link. For the considered setting, the transmission times and corresponding packet duration are tabulated in Table IV. The frame length computed is  $T = 1.6071$  s. Throughput  $S$  is computed from (14),  $S = 1.484$ . Note that the throughput computed in this case is significantly closer to the upper bound  $N/2$  (which is 1.5) as compared to the throughput computed in the previous section with fixed packet

duration and time slot length as shown in Fig. 3(b). The reason for an increase in the throughput from the previous case is the variability in the packet duration. From Fig. 6, it is clear that by varying the packet duration, the transmissions and receptions on each node can be scheduled in such a way that the total idle time is minimized while exploiting the large propagation delays. This results in the throughput gain. Note that all the receptions in Fig. 6 are interference free and the interfering packets are aligned with the duration in which the nodes are busy transmitting. However, the packet traffic demand was set to be one packet for each link for this example. The schedule found is optimal given the network geometry and the packet traffic demand. Do note that one of the packet duration on the link (2, 1) is 0. This essentially means that the transmission on this link does not take place. We did not constraint the problem in (19) with the requirement for any minimum duration for which each link needs to be served. This can be easily added by setting a positive lower bound on the packet duration.

- 2) *Nonnegligible packet headers:* Next, let us consider including the packet headers in the problem as explained in Section III-E. Note that inclusion of packet headers is needed if the packet duration values lesser than the packet header lengths are to be prevented in the resulting solution. The provision to include this in the problem allows us to find schedules such that the packet duration in the solution is at least greater than the packet header lengths. The propagation-delay constraints (4) and (5) after including packet header  $\tau_p$  are as follows:

$$t_{jk}^x + \beta T + (\tau_p + \tau_{jk}^x) + D_{ji} \leq t_{li}^y + D_{li} \quad (25)$$

or

$$t_{jk}^x + \beta T + D_{ji} \geq t_{li}^y + (\tau_p + \tau_{li}^y) + D_{li} \quad (26)$$

$\forall \{(j, k), (l, i) \in \mathcal{L}\}$ . The constraints are transformed and the corresponding MILFP is set up. The objective function does not need to be changed since the total time

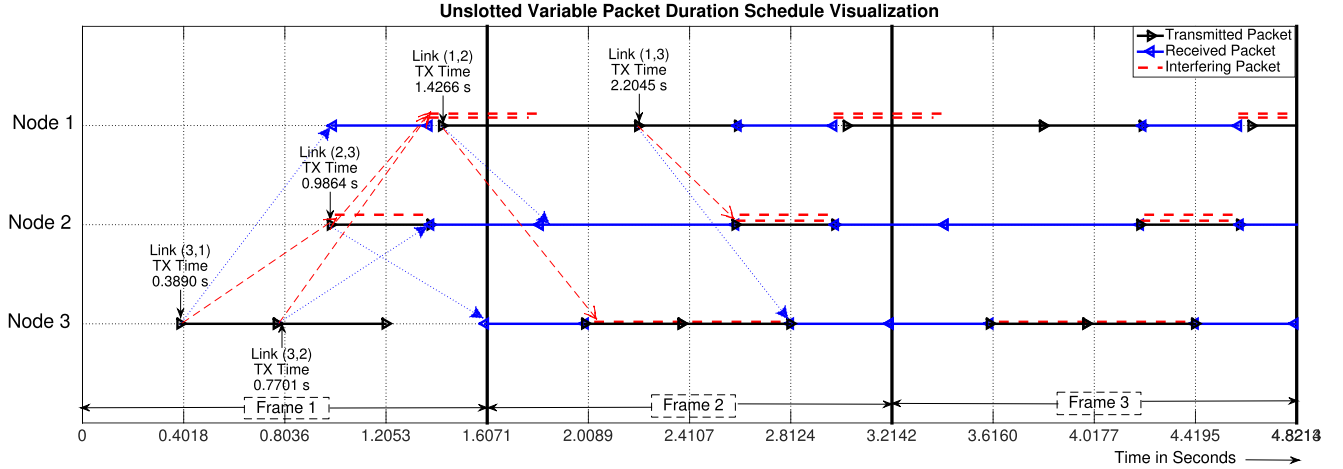


Fig. 6. Schedule visualization with variable packet duration. Note that there are no time slots and the transmission times and packet lengths are such that the total idle time is minimized. Throughput achieved is 1.484, which is significantly closer to the upper bound on the throughput.

TABLE V  
VARIABLE PACKET DURATION SOLUTION WITH PACKET HEADERS

Link	Transmission Start Time (s)	Payload Duration (s)
(1, 2)	0.0278	0.7579
(2, 1)	1.1947	0.0157
(2, 3)	1.2304	0.3768
(3, 2)	1.0142	0.3768
(1, 3)	0.8057	0.4125
(3, 1)	0.6330	0.3255

contributed by the packet headers of each transmission and reception is considered as the idle time and is a constant for known packet header duration. We set the packet header duration to be 20 ms and leave all other settings the same as in the previous section. The optimal solution with transmission times and the packet duration are computed and tabulated in Table V. The frame length in the solution is expected to be no lesser than its value computed without considering the packet headers. In this case, the frame length computed remains same,  $T = 1.6071$  s, however, with a different schedule as can be observed from the value of transmission times and the corresponding packet duration as shown in Table V. If we consider the channel utilization, the packet headers must be used in throughput computation and can be compared to the upper bound 1.5. The total channel utilization is 1.484 which is much closer to the upper bound. Also note that for this case the channel utilization remains the same to the case without considering the packet header duration, however with a different schedule (see Table V). The packet duration for the transmission on link (2, 1) in the case without the packet headers was 0 (see Table IV), while after considering the packet headers, on the same link (2, 1), the payload duration is 15.7 ms. Note that an optimal solution cannot be reached at by deducting the values of packet duration by the packet header duration and using the same schedule as Table IV, since this will lead to a negative packet duration on link (2, 1).

To summarize the results, the computed throughput for the considered sea-trial network geometry using the algorithms from [12] and [13] and MILFP (19) are shown in Fig. 3(b). Note that allowing variability in the packet duration resulted in a throughput much closer to the upper bound 1.5.

### B. Throughput Gain: Randomly Deployed Network Geometries

Consider an equilateral-triangle network with the propagation delay on each of the link set to 1 s. The optimal schedule and throughput for such a network geometry are known from [12]. For an equilateral-triangle network, the optimal throughput is 1.5 and can be achieved when the optimal schedule is adopted [12]. To generalize the results obtained for the three-node sea-trial network geometry, we randomly perturb the locations of the nodes in the equilateral-triangle network within a sphere of radius  $r$ . The random perturbations in the location of nodes affect the throughput. The coordinates of the node location are perturbed uniformly and the radius  $r$  is chosen such that it causes a change in the propagation delay of at most 0.4 s, i.e., the propagation delay on each link may lie between 0.8 and 1.2 s. The algorithms from [12] and [13] and MILFP (19) are used to compute the schedules and the corresponding throughput. The average throughput is computed over 100 such random instances. The comparison is shown in Fig. 7. Note that the results from [12] and [13] almost remain the same, however, the significant gain in the throughput is observed when the variability in the packet duration is allowed.

## VI. NETWORK GEOMETRIES WITH ARBITRARY TRAFFIC DEMANDS

In this section, we present optimal schedules for some network geometries, given arbitrary packet traffic demands with an objective to study the effect of packet traffic demands and to provide insights by comparing the similarities and differences with schedules computed in [12]. We elucidate these objectives here.

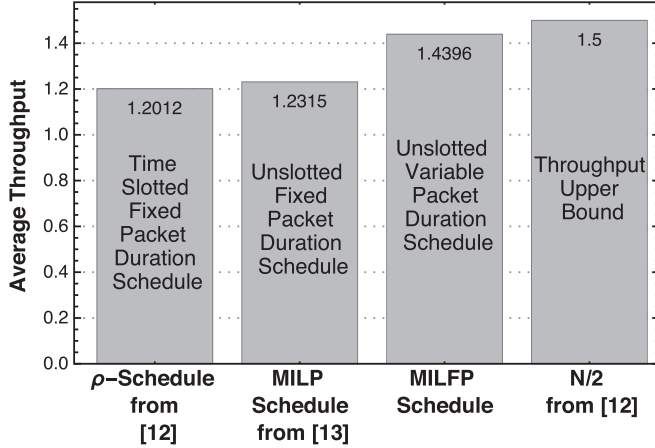


Fig. 7. Average throughput is computed over 100 network geometries with three nodes and six links to compare against the known upper bound on the throughput.

- 1) Effect of packet traffic demand: The throughput optimal schedules are already known for the network geometries that are considered here, from [12]. However, the packet traffic demands are not supported in [12]. We study the effect of including the traffic demands on these throughput optimal schedules. This setup is more practical, since, in reality, the traffic demands are derived from user requirements. The results in [12] only select those links for transmission which are throughput maximizing. However, the problem formulation in (19) allows us to select the links and the corresponding packet traffic demands. The lower bound on the packet duration can be set to a nonzero value to ensure minimum link fairness. This gives us control on the minimum fairness level to be maintained for all the links considered for scheduling. We demonstrate these features of the algorithm in this section.
- 2) Schedule matrix representation of MILFP solution: Since all the network geometries considered in this section for illustration have integer propagation delays among the links, the schedules found by solving (19) result in equal packet duration. Therefore, the solution can be represented in the form of a time-slotted schedule by simply setting the time slot length equal to the packet duration. This will be helpful in comparing the schedules computed with the time-slotted schedules in [12], which can be represented in the matrix form and are elucidated in Sections VI-A and VI-B. This provides insights on the similarity in the results obtained from [12] and the proposed MILFP algorithm.

#### A. Schedule Matrix

A schedule is denoted by matrix  $\mathbf{W}$  which determines the time slots in which each node in the network transmits and receives messages. Its entries are as follows.

- 1) If  $W_{j,t} = i > 0$ , then node  $j$  transmits a message to node  $i$  in time slot  $t$ .
- 2) If  $W_{j,t} = -i < 0$ , then node  $j$  receives a message from node  $i$  in time slot  $t$ .

- 3) If  $W_{j,t} = 0$ , then node  $j$  is idle during time slot  $t$ .

$nW_{j,t+T} = W_{j,t} \forall j, t$ , represents that the schedule is of frame length  $T$ . Therefore, it can be written as a matrix of order  $N \times T$  denoted by  $\mathbf{W}^{(T)}$  (see [12, Sec. III-B] for details). Note that solving the MILFP presented in (19) can be represented in the form of the schedule matrix only because the solution for the considered network geometries in this section results in equal packet duration and thus provides an opportunity to compare the solutions and appreciate the similarity and differences among them.

#### B. Illustrative Network Geometries

For each network geometry, we consider two different sets of packet traffic demands denoted by  $\Lambda^1$  and  $\Lambda^2$ . Each set  $\Lambda^1$  and  $\Lambda^2$  contains the packet traffic demand for each link  $l \in \mathcal{L}$ . For example,  $\Lambda_l^1$  packets/frame is the packet traffic demand on link  $l$  from the first set and  $\Lambda_l^2$  packets/frame is the packet traffic demand on link  $l$  from the second set. Table VI lists the arbitrarily set packet traffic demands for the networks considered. There are six links to be scheduled for all three networks as shown in the first column of Table VI. For example,  $\Lambda_{(1,2)}^2 = 3$  for the equilateral-triangle network in Table VI implies that there must be three packet transmissions per frame on link (1, 2).

1) *Equilateral Triangle*: Consider an equilateral-triangle-shaped network geometry with the propagation delay between the links set as 1 s. We consider two different sets of packet traffic demands as shown in Table VI. The delay matrix<sup>2</sup> for a three-node equilateral-triangle network geometry is

$$\mathbf{D} = \begin{bmatrix} 0 & 1 & 1 \\ 1 & 0 & 1 \\ 1 & 1 & 0 \end{bmatrix}$$

and the optimal schedules computed by solving (19) for the packet traffic demands  $\Lambda_l^1$  and  $\Lambda_l^2$  are represented in Table VII. The packet transmission times and the corresponding packet duration on each of the six links considered are presented in appropriate columns of Table VII. Moreover, the solution is also represented in the form of the schedule matrix  $\mathbf{W}$  (shown in the last row of Table VII) to compare it with the solution in [12].

- 1)  $\Lambda_l^1$  packets/frame: The six links considered must be scheduled once in the frame. The solution found is listed in Table VII, and the frame length computed is  $T = 4$ . The transmission times and packet duration listed in Table VII are represented in the form of the schedule matrix denoted as  $\mathbf{W}^{(4)}$ . Note that there are six positive entries per frame of length  $T = 4$  s indicating six successful transmissions per frame, and hence the throughput is computed as  $S = (6/4) = 1.5$ . The throughput optimal schedule computed in [12] is the same schedule as shown in Table VII

<sup>2</sup>Note, in this section, the elements of the delay matrix are in units of seconds and not in units of time slot length as considered in Section V-A1. We present the propagation delays in the form of the delay matrix only for maintaining uniformity with the representation in [12].

TABLE VI  
ARBITRARY PACKET TRAFFIC DEMANDS FOR ILLUSTRATIVE NETWORK GEOMETRIES CONSIDERED

Link	Equilateral Triangle			Isosceles Triangle			Linear Network		
	Propagation Delay (s)	Packet Traffic Demand		Propagation Delay (s)	Packet Traffic Demand		Propagation Delay (s)	Packet Traffic Demand	
		$\Lambda_l^1$ pkts/frame	$\Lambda_l^2$ pkts/frame		$\Lambda_l^1$ pkts/frame	$\Lambda_l^2$ pkts/frame		$\Lambda_l^1$ pkts/frame	$\Lambda_l^2$ pkts/frame
(1, 2)	1	1	3	1	1	1	1	1	2
(2, 1)	1	1	1	1	1	2	1	1	1
(2, 3)	1	1	2	2	1	1	1	1	2
(3, 2)	1	1	2	2	1	2	1	1	1
(1, 3)	1	1	1	2	1	1	2	1	2
(3, 1)	1	1	3	2	1	2	2	1	1

TABLE VII  
OPTIMAL SCHEDULES FOR EQUILATERAL-TRIANGLE NETWORK GEOMETRY

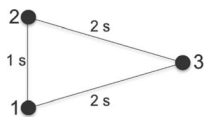
Link	$\Lambda_l^1$ packets/frame		$\Lambda_l^2$ packets/frame	
	Transmission Time (s)	Packet Duration (s)	Transmission Time (s)	Packet Duration (s)
(1, 2)	$t_{12}^1 = 0$	$\tau_{12}^1 = 1$	$t_{12}^1 = 3, t_{12}^2 = 6, t_{12}^3 = 7$	$\tau_{12}^1 = 1, \tau_{12}^2 = 1, \tau_{12}^3 = 1$
(2, 1)	$t_{21}^1 = 0$	$\tau_{21}^1 = 1$	$t_{21}^1 = 3$	$\tau_{21}^1 = 1$
(2, 3)	$t_{23}^1 = 3$	$\tau_{23}^1 = 1$	$t_{23}^1 = 1, t_{23}^2 = 5$	$\tau_{23}^1 = 1, \tau_{23}^2 = 1$
(3, 2)	$t_{32}^1 = 1$	$\tau_{32}^1 = 1$	$t_{32}^1 = 1, t_{32}^2 = 5$	$\tau_{32}^1 = 1, \tau_{32}^2 = 1$
(1, 3)	$t_{13}^1 = 2$	$\tau_{13}^1 = 1$	$t_{13}^1 = 2$	$\tau_{13}^1 = 1$
(3, 1)	$t_{31}^1 = 2$	$\tau_{31}^1 = 1$	$t_{31}^1 = 0, t_{31}^2 = 4, t_{31}^3 = 8$	$\tau_{31}^1 = 1, \tau_{31}^2 = 1, \tau_{31}^3 = 1$
<div style="display: flex; justify-content: space-around;"> <div> <p><b>Equivalent Schedule Matrix</b></p> <math display="block">\mathbf{W}^{(4)} = \begin{bmatrix} 2 &amp; -2 &amp; 3 &amp; -3 \\ 1 &amp; -1 &amp; -3 &amp; 3 \\ -2 &amp; 2 &amp; 1 &amp; -1 \end{bmatrix}</math> <p><b>Throughput</b> <math>\Rightarrow S = \frac{6}{4} = 1.5</math></p> </div> <div> <p><b>Equivalent Schedule Matrix</b></p> <math display="block">\mathbf{W}^{(9)} = \begin{bmatrix} -3 &amp; -3 &amp; 3 &amp; 2 &amp; -2 &amp; -3 &amp; 2 &amp; 2 &amp; 0 \\ 0 &amp; 3 &amp; -3 &amp; 1 &amp; -1 &amp; 3 &amp; -3 &amp; -1 &amp; -1 \\ 1 &amp; 2 &amp; -2 &amp; -1 &amp; 1 &amp; 2 &amp; -2 &amp; 0 &amp; 1 \end{bmatrix}</math> <p><b>Throughput</b> <math>\Rightarrow S = \frac{12}{9} = 1.33</math></p> </div> </div>				

for the equilateral triangle where only the throughput-maximizing links are chosen. This shows that selection of  $\Lambda_l^1$  packet traffic demand is throughput optimal for the considered equilateral-triangle network geometry.

- 2)  $\Lambda_l^2$  packets/frame: For this case, the six links are scheduled as many times as represented in the column  $\Lambda_l^2$  packets/frame of Table VI. The transmission times and packet duration are shown in Table VII along with the equivalent schedule matrix  $\mathbf{W}^{(9)}$ . The frame length computed is  $T = 9$ . The formulation allows us to compute such schedules with arbitrary traffic demands which is not possible using the algorithm from [12]. Note that the schedule computed has three idle slots and the throughput computed is 1.33, which is although greater than 1, which is lesser than the throughput upper bound.

2) *Isosceles Triangle*: Next, we consider an isosceles-triangle-shaped network geometry with the delay matrix as shown below:

$$\mathbf{D} = \begin{bmatrix} 0 & 1 & 2 \\ 1 & 0 & 2 \\ 2 & 2 & 0 \end{bmatrix}$$



We consider again two different sets of packet traffic demands as shown in Table VI.


- 1)  $\Lambda_l^1$  packets/frame: Again the six links considered must be scheduled once in the frame for this case. The frame length computed is  $T = 4$  and throughput  $S$  is 1.5. The equivalent schedule matrix along with the MILFP solution is shown in Table VIII. The schedule  $\mathbf{W}^{(4)}$  computed for this case is significantly different from the optimal schedule found for the same network geometry in [12]. Although both the schedules are throughput optimal, the difference is the frame length.
- 2)  $\Lambda_l^2$  packets/frame: Next, we consider each of the six links to be scheduled as per the packet traffic demand listed in  $\Lambda_l^2$  column of Table VI. The lower bound ( $\tau_{lb}$ ) on the packet duration is set to 1 s for this case to ensure that each link transmits at least 1 s. We expect to find schedules in which the packet traffic demand is satisfied along with the minimum packet duration requirement. The frame length is computed to be  $T = 7$ , and the optimal solution is represented in Table VIII. Note that all the six links considered are active for 1 s and the packet traffic demand is also satisfied, i.e., the links (2, 1), (3, 2), and (3, 1) all transmit twice in the frame along with the rest of the links, which transmitted one packet per frame as required.



TABLE VIII  
OPTIMAL SCHEDULES FOR ISOSCELES-TRIANGLE NETWORK GEOMETRY

Link	$\Lambda_l^1$ packets/frame		$\Lambda_l^2$ packets/frame	
	Transmission Time (s)	Packet Duration (s)	Transmission Time (s)	Packet Duration (s)
(1, 2)	$t_{12}^1 = 0$	$\tau_{12}^1 = 1$	$t_{12}^1 = 0$	$\tau_{12}^1 = 1$
(2, 1)	$t_{21}^1 = 2$	$\tau_{21}^1 = 1$	$t_{21}^1 = 0, t_{21}^2 = 2$	$\tau_{21}^1 = 1, \tau_{21}^2 = 1$
(2, 3)	$t_{23}^1 = 3$	$\tau_{23}^1 = 1$	$t_{23}^1 = 3$	$\tau_{23}^1 = 1$
(3, 2)	$t_{32}^1 = 2$	$\tau_{32}^1 = 1$	$t_{32}^1 = 2, t_{32}^2 = 4$	$\tau_{32}^1 = 1, \tau_{32}^2 = 1$
(1, 3)	$t_{13}^1 = 1$	$\tau_{13}^1 = 1$	$t_{13}^1 = 6$	$\tau_{13}^1 = 1$
(3, 1)	$t_{31}^1 = 0$	$\tau_{31}^1 = 1$	$t_{31}^1 = 0, t_{31}^2 = 3$	$\tau_{31}^1 = 1, \tau_{31}^2 = 1$
<b>Equivalent Schedule Matrix</b>			<b>Equivalent Schedule Matrix</b>	
$\mathbf{W}^{(4)} = \begin{bmatrix} 2 & 3 & -3 & -2 \\ -3 & -1 & 1 & 3 \\ 1 & -2 & 2 & -1 \end{bmatrix}$			$\mathbf{W}^{(7)} = \begin{bmatrix} 2 & -2 & -3 & -2 & 0 & -3 & 3 \\ 1 & -1 & 1 & 3 & -3 & 0 & -3 \\ 1 & -1 & 2 & 1 & 2 & -2 & 0 \end{bmatrix}$	
<b>Throughput</b>			<b>Throughput</b>	
$\Rightarrow S = \frac{6}{4} = 1.5$			$\Rightarrow S = \frac{9}{7} = 1.2857$	

3) *Linear Network*: Now we consider a three-node linear network with the delay matrix:

$$\mathbf{D} = \begin{bmatrix} 0 & 1 & 2 \\ 1 & 0 & 1 \\ 2 & 1 & 0 \end{bmatrix}$$


The different packet traffic demands are shown in Table VI. The corresponding schedule is computed again by solving (19).

- 1)  $\Lambda_l^1$  packets/frame: For this case, we compute the schedules with both  $\tau_{lb} = 0$  and 1 s. In Table IX, we present the schedule with lower bound  $\tau_{lb}$  set to 0. When  $\tau_{lb}$  is set to 1 s, the optimal schedule matrix computed is

$$\mathbf{W}^{(6)} = \begin{bmatrix} 2 & -2 & 3 & 3 & -3 & -3 \\ 1 & -1 & -3 & 0 & 0 & 3 \\ -2 & 2 & 1 & 1 & -1 & -1 \end{bmatrix}$$

$$\Rightarrow S = \frac{8}{6} = 1.33. \quad (27)$$

The schedule computed is significantly different from the result in [12]. The schedule from [12] for the same linear network is the same as shown in Table IX. Note that for the schedule from [12], the links (2, 1) and (3, 2) are not scheduled. The reason is that the algorithm in [12] only selects the throughput-maximizing links. However, we solve the MILFP (19) by setting  $\tau_{lb} = 1$  s and  $\Lambda_l^1$  packets/frame on each link, to make sure that all the links are scheduled at least once with packet duration of at least 1 s. Therefore, we see that links (2, 1) and (3, 2) are scheduled with a packet duration of at least 1 s in  $\mathbf{W}^{(6)}$  as shown in (27).

- 2)  $\Lambda_l^2$  packets/frame: Similarly, we also present the MILFP solution and the equivalent schedule matrix with  $\tau_{lb} = 1$  s for this case as shown in Table IX. The frame length computed is  $T = 8$ , with throughput  $S = 1.12$ .

These examples demonstrate that the control provided by this formulation is necessary to compute useful schedules for many application scenarios with different traffic demands.

## VII. SCALABILITY AND COMPLEXITY ANALYSIS

In Section V, we considered a UWA network with single collision domain and demonstrated that unslotted schedules with variable packet duration result in throughput closer to the upper bound and outperform the state-of-the-art centralized algorithms presented in [12] and [13]. The proposed MILFP is a centralized algorithm and schedules are computed offline. The maximum network size (in terms of the number of nodes and links) for which MILFP can be solved in a reasonable amount of time is of interest. To study the scalability of the algorithm with the number of nodes and links in the network, we compute schedules for much larger multihop networks. The proposed algorithm is general enough to be used for finding schedules for multihop UWA networks with multiple partially overlapping collision domains. We consider multihop multiline grid networks (also considered in [14]) and compute the schedules using (19) as the number of nodes in the network increases. Multihop multiline grid topology consists of parallel lines with regularly placed nodes. Messages originate from the first node on each line and are destined to the final node on the same line. Intermediate nodes act as relay nodes which receive the incoming packets, decode them, and retransmit them to the next hop until they reach the final destination node. The spacing between neighboring nodes on the same line corresponds to a propagation delay of 1 s and the distance separating every two adjacent lines correspond to the propagation delay of 2 s (see [14] for details). The ratio of interference range to the communication range  $\alpha$  is set to 2 and hence a transmission on a link with propagation delay 1 s among them interferes with the node on the adjacent line to which the propagation delay is 2 s. For a multihop network, multiple partially overlapping collision domains exist and the problem formulation presented in Section III allows us to enumerate the propagation-delay constraints for such case.

The classical approach for solving MILP with binary variables used in Algorithm 1 is the tree search by a Branch &

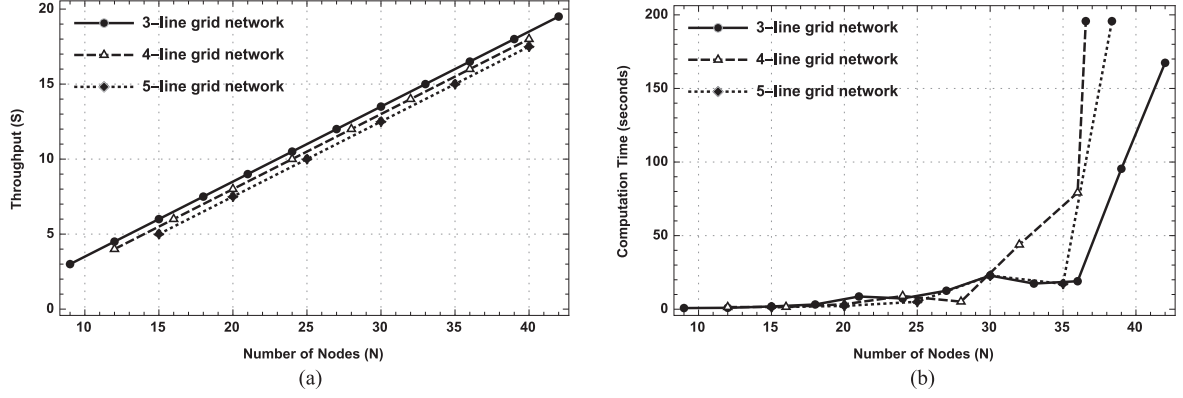


Fig. 8. Throughput and computation time as a function of the number of nodes in a multihop multiline grid network using MILFP. (a) Scalability with the number of nodes and links. (b) Computation time with the number of nodes and links.

TABLE IX  
OPTIMAL SCHEDULES FOR LINEAR NETWORK GEOMETRY

Link	$\Lambda_l^1$ packets/frame		$\Lambda_l^2$ packets/frame	
	Transmission Time (s)	Packet Duration (s)	Transmission Time (s)	Packet Duration (s)
(1, 2)	$t_{12}^1 = 1$	$\tau_{12}^1 = 1$	$t_{12}^1 = 0, t_{12}^2 = 6$	$\tau_{12}^1 = 1, \tau_{12}^2 = 1$
(2, 1)	$t_{21}^1 = 1$	$\tau_{21}^1 = 0$	$t_{21}^1 = 0$	$\tau_{21}^1 = 1$
(2, 3)	$t_{23}^1 = 0$	$\tau_{23}^1 = 1$	$t_{23}^1 = 3, t_{23}^2 = 6$	$\tau_{23}^1 = 1, \tau_{23}^2 = 1$
(3, 2)	$t_{32}^1 = 2$	$\tau_{32}^1 = 0$	$t_{32}^1 = 1$	$\tau_{32}^1 = 1$
(1, 3)	$t_{13}^1 = 0$	$\tau_{13}^1 = 1$	$t_{13}^1 = 3, t_{13}^2 = 4$	$\tau_{13}^1 = 1, \tau_{13}^2 = 1$
(3, 1)	$t_{31}^1 = 0$	$\tau_{31}^1 = 1$	$t_{31}^1 = 3$	$\tau_{31}^1 = 1$
<b>Equivalent Schedule Matrix</b>				
$\mathbf{W}^{(3)} = \begin{bmatrix} 3 & 2 & -3 \\ 3 & 0 & -1 \\ 1 & -2 & -1 \end{bmatrix}$			$\mathbf{W}^{(8)} = \begin{bmatrix} 2 & -2 & 0 & 3 & 3 & -3 & 2 & 0 \\ 1 & -1 & -3 & 3 & 0 & 0 & 3 & -1 \\ 0 & 2 & 0 & 1 & -2 & -1 & -1 & -2 \end{bmatrix}$	
<b>Throughput</b> $\Rightarrow S = \frac{4}{3} = 1.33$			<b>Throughput</b> $\Rightarrow S = \frac{9}{8} = 1.12$	

Bound algorithm with linear programming relaxation, which generally has an exponential complexity in the worst case. An indicator that can be quantified for indicating the complexity of the problem formulated is the number of binary variables  $b$  required. We can compute  $b$  in terms of the number of nodes  $N$ , the number of links to be scheduled  $|\mathcal{L}|$ , and the packet traffic demand  $\Lambda_{jk}$  on each link  $(j, k) \in \mathcal{L}$ . The number of binary variables depends on the number of link pairs  $(j, k), (l, i) \in \mathcal{L}$  such that the condition  $D_{ji} \leq \alpha D_{jk}$  is satisfied. For a single collision domain network, any transmission on a particular link  $(j, k)$  causes interference to all other nodes. Therefore, the case of single collision domain presents the worst case for which the number of binary variables is computed as follows:

$$b = (2\beta + 1) \left( \sum_{\forall (j,k) \in \mathcal{L}} \left( \sum_{\substack{\forall (l,i) \in \mathcal{L} \\ (l,i) \neq (j,k)}} \Lambda_{jk} \Lambda_{li} \right) \right) \quad (28)$$

where  $\beta$  takes the maximum value for which the propagation-delay constraints are enumerated in the MILFP (19). It is worth noting that a number of binary variables  $b$  scale on the order of the square of the number of links in  $\mathcal{L}$ . To see this, consider the case of a single collision domain network with packet traffic demand  $\Lambda_{jk} = 1$  packet/frame  $\forall (j, k) \in \mathcal{L}$ . For this case,

TABLE X  
LINK PROPAGATION DELAYS

Link	Sea-Trial Network (s)	Isosceles Triangle (s)
(1, 2)	0.3890	1
(2, 1)	0.3890	1
(2, 3)	0.6130	2
(3, 2)	0.6130	2
(1, 3)	0.6052	2
(3, 1)	0.6052	2

with  $\beta = 1$  and using (28), we compute the number of binary variables to be

$$b = 3|\mathcal{L}|(|\mathcal{L}| - 1). \quad (29)$$

We vary the number of nodes from nine to 42 for the grid networks considered with three lines, four lines, and five lines. Note that for an  $N$  node multihop multiline grid network with  $\eta$  parallel lines, there are  $N - \eta$  links to be scheduled. The MILFP (19) is solved for a minimum of six links to a maximum of 39 links. The optimal solution computed always corresponds to the maximum achievable throughput [see Fig. 8(a)] for the network and can be verified from the results in [14]. For the case with

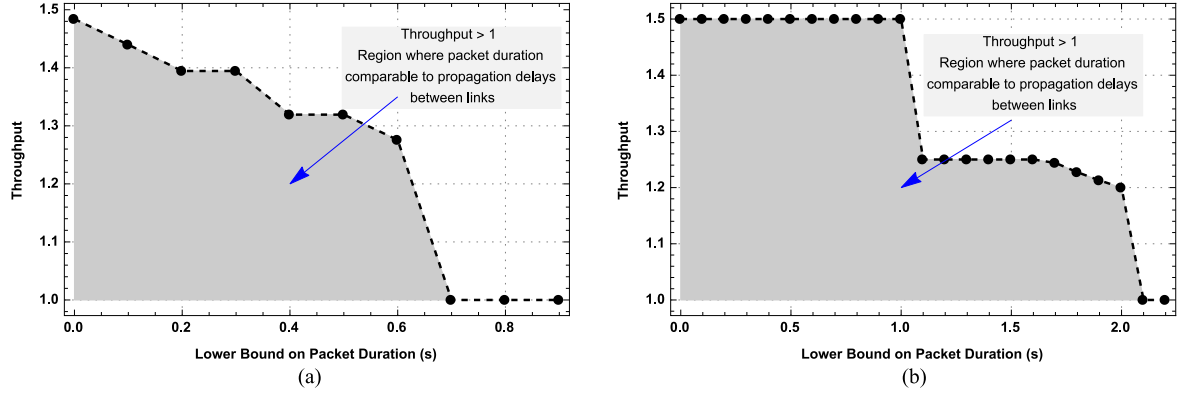


Fig. 9. Throughput corresponding to the schedules computed for network geometry considered. Upper bound on throughput is achieved when the lower bound on packet duration is set to 0 and hence supports the proposition that for an arbitrary network geometry the throughput upper bound is computed by solving (19) with  $\tau_{lb} = 0$ . (a) Sea-trial network geometry. (b) Isosceles-triangle network geometry.

$N = 42$  nodes and 39 links, the number of binary variables  $b$  is computed to be 549, the number of constraints listed was 1176, and the total number of variables in the problem was 629. We use MOSEK optimizer with MATLAB on an iMac with 2.5-GHz Intel Core i5 quad-core processor to solve the MILP in Algorithm 1. The computation time in seconds for each case is plotted in Fig. 8(b) and can be seen that the optimal schedules are computed in reasonable time for all these networks. For 42 nodes with 39 links the MILFP converges to the optimal solution in 167.42 s. Also, note that, in practice, UWA networks are not as large as considered in this analysis and hence the proposed centralized algorithm provides a good alternative for providing better benchmarks in computing throughput-maximizing schedules. The comparison of the proposed MILFP solution for such large multihop multiline grid networks with the time-slotted strategy in [12] is presented in [32].

### VIII. REGION OF OPERATION: EXPLOITING LARGE PROPAGATION DELAYS

In the previous sections, we have demonstrated that by allowing variability in the packet duration, significant throughput gains can be achieved, and presented that the proposed MILFP outperforms other state-of-the-art centralized algorithms. However, under what conditions can we exploit large propagation delays to achieve throughput gains? In this section, we show that only when the packet duration used for transmissions is comparable to the link propagation delay in the network, achievable throughput is greater than what can be achieved in the terrestrial wireless networks with negligible propagation delay. We study the region in which the network must be operated in, to take advantage of the large propagation delay.

*Proposition:* Assuming the frame length of a schedule to be greater than the girth of a single collision domain network, i.e.,  $T > G$ , the upper bound on the throughput of any arbitrary network geometry is found by solving (19) with the lower bound  $\tau_{lb}$  on the packet duration set to 0.

*Proof:* Let the feasible set for problem (19) be denoted by  $\mathcal{F}$  when  $\tau_{lb} = 0$ , and denote the feasible set by  $\mathcal{F}'$  when  $\tau_{lb} > 0$ . Since the feasible set  $\mathcal{F}$  with relaxed lower bound includes the

feasible set  $\mathcal{F}'$  with some positive lower bound, i.e.,

$$\mathcal{F}' \subseteq \mathcal{F} \quad (30)$$

the optimal value of the problem with relaxation on the lower bound must be always less than or equal to the optimal value of the problem with some set positive lower bound. In other words, the throughput computed with  $\tau_{lb} > 0$  can be no greater than the throughput computed with  $\tau_{lb} = 0$ . ■

Next, we study the region in which the network must be operated to achieve the throughput gains due to the presence of large propagation delays. To study this, we consider two network geometries: a sea-trial network geometry shown in Fig. 2 and an isosceles-triangle-shaped network geometry. The propagation delay corresponding to the links is as shown in Table X. We vary the lower bound ( $\tau_{lb}$ ) on packet duration and compute the schedules and the corresponding throughput for both network geometries considered. The resulting throughput is plotted and shown in Fig. 9. We present the following observations and insights from the simulation results.

- 1) For both network geometries, the highest throughput is achieved when  $\tau_{lb} = 0$  and supports the proposition. The value of throughput is 1.484 for the sea-trial network geometry and is 1.5 for the isosceles-triangle-shaped network geometry.
- 2) Throughput is a nonincreasing function of the lower bound on the packet duration. For example, it remains at 1.5 until the value of  $\tau_{lb} = 1$ , in the case of isosceles-triangle-shaped network geometry and then reduces further as the lower bound is increased.
- 3) For terrestrial wireless networks using radio-frequency waves, the highest throughput that can be achieved is not greater than 1. In Fig. 9(a) and (b), we see that the shaded region is where the throughput is higher than the throughput achievable in terrestrial wireless networks.
- 4) Throughput reduces to 1 for both network geometries when

$$\tau_{lb} > \max_{\forall(j,k) \in \mathcal{L}} D_{jk}. \quad (31)$$

So, only when the packet durations are less than the maximum propagation delay in the network, the throughput gain is possible. In fact, this is the definition of the large propagation delay, since large propagation delays are relative to the transmission duration considered.

## IX. CONCLUSION

We formulated an optimization problem with the goal of finding throughput-maximizing schedules. We exploited large propagation delays by minimizing the fractional idle time in a frame, given the packet traffic demands on the links considered in a practical UWA network. In contrast to the approach where the minimum length schedules are computed by minimizing the frame length, we considered the fractional idle time to allow variability in the packet transmission duration. We presented and visualized the time-slotted fixed packet duration solution and compared it with the proposed MILFP solution resulting in schedules with no time slots and variable packet duration. The variability in the packet duration was crucial in achieving the throughput gain, thereby resulting in throughput closer to the upper bound  $N/2$ . The proposed algorithm outperformed the existing state-of-the-art methods to find schedules exploiting the large propagation delays. We computed schedules for some illustrative network geometries with arbitrary packet traffic demands and compared it with the previous work. The centralized algorithm proposed is used to compute schedules for multihop multiline grid networks to demonstrate the scalability of the algorithm. We studied the operating region for UWA networks in which throughput gains due to the large propagation delays can be achieved. We presented throughput behavior, as the lower bound on packet duration is varied. This study provided insights and quantified the regions where the propagation delays and transmission duration are comparable. The results are presented to confirm the benefits of unslotted variable packet duration schedules in maximizing throughput for arbitrary UWA networks.

## REFERENCES

- [1] I. F. Akyildiz, D. Pompili, and T. Melodia, "Underwater acoustic sensor networks: Research challenges," *Ad Hoc Netw.*, vol. 3, no. 3, pp. 257–279, 2005.
- [2] J. Kong, J.-H. Cui, D. Wu, and M. Gerla, "Building underwater ad-hoc networks and sensor networks for large scale real-time aquatic applications," in *Proc. IEEE Military Commun. Conf.*, 2005, pp. 1535–1541.
- [3] M. Chitre, S. Shahabudeen, and M. Stojanovic, "Underwater acoustic communications and networking: Recent advances and future challenges," *Mar. Technol. Soc. J.*, vol. 42, no. 1, pp. 103–116, 2008.
- [4] J. Heidemann, M. Stojanovic, and M. Zorzi, "Underwater sensor networks: Applications, advances and challenges," *Philos. Trans. Roy. Soc. Lond. A, Math. Phys. Eng. Sci.*, vol. 370, no. 1958, pp. 158–175, 2012.
- [5] R. J. Urick, *Principles of Underwater Sound for Engineers*. New York, NY, USA: Tata McGraw-Hill Education, 1967.
- [6] J. Heidemann, W. Ye, J. Wills, A. Syed, and Y. Li, "Research challenges and applications for underwater sensor networking," in *Proc. IEEE Wireless Commun. Netw. Conf.*, vol. 1, 2006, pp. 228–235.
- [7] J. Rice *et al.*, "Evolution of seabed underwater acoustic networking," in *Proc. MTS/IEEE OCEANS Conf. Exhib.*, vol. 3, 2000, pp. 2007–2017.
- [8] G. Zhongwen, L. Zhengbao, and H. Feng, "USS-TDMA: Self-stabilizing TDMA algorithm for underwater wireless sensor network," in *Proc. Int. Conf. Comput. Eng. Technol.*, vol. 1, 2009, pp. 578–582.
- [9] H.-H. Ng, W.-S. Soh, and M. Motani, "A bidirectional-concurrent MAC protocol with packet bursting for underwater acoustic networks," *IEEE J. Ocean. Eng.*, vol. 38, no. 3, pp. 547–565, 2013.
- [10] J. Ma and W. Lou, "Interference-aware spatio-temporal link scheduling for long delay underwater sensor networks," in *Proc. 8th Annu. IEEE Commun. Soc. Conf. Sensor Mesh Ad Hoc Commun. Netw.*, 2011, pp. 431–439.
- [11] Y. Noh, P. Wang, U. Lee, D. Torres, and M. Gerla, "DOTS: A propagation delay-aware opportunistic MAC protocol for underwater sensor networks," in *Proc. 18th IEEE Int. Conf. Network Protocols*, 2010, pp. 183–192.
- [12] M. Chitre, M. Motani, and S. Shahabudeen, "Throughput of networks with large propagation delays," *IEEE J. Ocean. Eng.*, vol. 37, no. 4, pp. 645–658, 2012.
- [13] C.-C. Hsu, M.-S. Kuo, C.-F. Chou, and K. C.-J. Lin, "The elimination of spatial-temporal uncertainty in underwater sensor networks," *IEEE/ACM Trans. Netw.*, vol. 21, no. 4, pp. 1229–1242, 2013.
- [14] S. Lmai, M. Chitre, C. Laot, and S. Houcke, "TDMA-based MAC transmission schedules in multihop grid ad hoc underwater acoustic networks," in *Proc. IEEE Underwater Commun. Netw.*, 2014, doi: 10.1109/UComms.2014.7017131.
- [15] H. Zeng, Y. T. Hou, Y. Shi, W. Lou, S. Kompella, and S. F. Midkiff, "SHARK-IA: An interference alignment algorithm for multi-hop underwater acoustic networks with large propagation delays," in *Proc. Int. Conf. Underwater Netw. Syst.*, 2014, p. 6.
- [16] K. Kredo *et al.*, "STUMP: Exploiting position diversity in the staggered TDMA underwater MAC protocol," in *Proc. IEEE INFOCOM*, 2009, pp. 2961–2965.
- [17] B. Peleato and M. Stojanovic, "Distance aware collision avoidance protocol for ad-hoc underwater acoustic sensor networks," *IEEE Commun. Lett.*, vol. 11, no. 12, pp. 1025–1027, 2007.
- [18] X. Guo, M. R. Frater, and M. J. Ryan, "Design of a propagation-delay-tolerant MAC protocol for underwater acoustic sensor networks," *IEEE J. Ocean. Eng.*, vol. 34, no. 2, pp. 170–180, 2009.
- [19] F. L. Presti, C. Petrioli, R. Petrocchia, and A. Shashaj, "A scalable analytical framework for deriving optimum scheduling and routing in underwater sensor networks," in *Proc. IEEE 9th Int. Conf. Mobile Adhoc Sensor Syst.*, 2012, pp. 127–135.
- [20] R. Diamant, G. N. Shirazi, and L. Lampe, "Robust spatial reuse scheduling in underwater acoustic communication networks," *IEEE J. Ocean. Eng.*, vol. 39, no. 1, pp. 32–46, 2014.
- [21] Y. Han and Y. Fei, "TARS: A traffic-adaptive receiver-synchronized MAC protocol for underwater sensor networks," in *Proc. IEEE 23rd Int. Symp. Model. Anal. Simul. Comput. Telecommun. Syst.*, 2015, doi: 10.1109/MASCOTS.2015.10.
- [22] Z. Guan, T. Melodia, and D. Yuan, "Stochastic channel access for underwater acoustic networks with spatial and temporal interference uncertainty," in *Proc. 7th ACM Int. Conf. Underwater Netw. Syst.*, 2012, p. 18.
- [23] P. Gupta and P. R. Kumar, "The capacity of wireless networks," *IEEE Trans. Inf. Theory*, vol. 46, no. 2, pp. 388–404, 2000.
- [24] S. Lee and I. E. Grossmann, "New algorithms for nonlinear generalized disjunctive programming," *Comput. Chem. Eng.*, vol. 24, no. 9, pp. 2125–2141, 2000.
- [25] I. E. Grossmann and F. Trespalcacios, "Systematic modeling of discrete-continuous optimization models through generalized disjunctive programming," *AIChE J.*, vol. 59, no. 9, pp. 3276–3295, 2013.
- [26] L. A. Wolsey and G. L. Nemhauser, *Integer and Combinatorial Optimization*. New York, NY, USA: Wiley, 2014, ch. 1, p. 12.
- [27] D. Yue, G. Guillén-Gosálbez, and F. You, "Global optimization of large-scale mixed-integer linear fractional programming problems: A reformulation-linearization method and process scheduling applications," *AIChE J.*, vol. 59, no. 11, pp. 4255–4272, 2013.
- [28] S. Boyd and L. Vandenberghe, *Convex Optimization*. Cambridge, U.K.: Cambridge Univ. Press, 2004, ch. 4, p. 157.
- [29] Z. Zhong and F. You, "Parametric algorithms for global optimization of mixed-integer fractional programming problems in process engineering," in *Proc. IEEE Amer. Control Conf.*, 2014, pp. 3609–3614.
- [30] M. Chitre, I. Topor, and T.-B. Koay, "The UNET-2 modem—An extensible tool for underwater networking research," in *Proc. IEEE OCEANS Conf.*, 2012, DOI: 10.1109/OCEANS-Yeosu.2012.6263431.
- [31] M. Chitre, I. Topor, R. Bhatnagar, and V. Pallayil, "Variability in link performance of an underwater acoustic network," in *Proc. MTS/IEEE OCEANS-Bergen Conf.*, 2013, DOI: 10.1109/OCEANS-Bergen.2013.6607953.
- [32] P. Anjani and M. Chitre, "Unslotted transmission schedules for practical underwater acoustic multihop grid networks with large propagation delays," in *Proc. IEEE Underwater Commun. Netw.*, 2016, DOI: 10.1109/UComms.2016.7583429.





**Prasad Anjangi** (S'16) received the B.Eng. degree in electronics and instrumentation engineering from Andhra University, Andhra Pradesh, India, in 2007 and the M.Eng. degree in biomedical engineering from the Indian Institute of Technology (IIT), Bombay, India, in 2009. Currently, he is working toward the Ph.D. degree in the Department of Electrical and Computer Engineering, National University of Singapore (NUS), Singapore.

He worked in semiconductor industries with Atmel and STMicroelectronics as Firmware and Senior Design Engineer, respectively, from 2009 to 2012. His current research interests include underwater acoustic communications, networking protocol design, and autonomous underwater vehicles.



**Mandar Chitre** received the B.Eng. and M.Eng. degrees in electrical engineering from the National University of Singapore (NUS), Singapore, the M.Sc. degree in bioinformatics from the Nanyang Technological University (NTU), Singapore, and the Ph.D. degree from NUS.

From 1997 to 1998, he worked with the ARL, NUS. From 1998 to 2002, he headed the technology division of a regional telecommunications solutions company. In 2003, he rejoined ARL, initially as the Deputy Head (Research) and is now the Head of the laboratory. He also holds a joint appointment with the Department of Electrical and Computer Engineering at NUS as an Associate Professor. His current research interests are underwater communications, autonomous underwater vehicles, and acoustic signal processing.

Dr. Chitre has served on the technical program committees of the IEEE OCEANS, WUWNet, DTA, and OTC conferences and has served as reviewer for numerous international journals. He was the chairman of the student poster committee for IEEE OCEANS'06 in Singapore, and the chairman for the IEEE Singapore AUV Challenge 2013. He is currently the IEEE Ocean Engineering Society Technology Committee Co-Chair of underwater communication, navigation & positioning, and on the editorial board of the IEEE JOURNAL OF OCEANIC ENGINEERING and the IEEE COMMUNICATIONS MAGAZINE.